Internal Memo

TO

CC

SUBJECT
Mode of Action of Dispersants – Report on SAXS measurements at DESY

18.06.2013

Dr. Michael Klostermann
Phone +49 201 173-3277
michael.mk.klostermann@evonik.com

The scope of this research project is to gain a deeper understanding for the mode of action of dispersing agents. To study both the adsorption behavior of dispersants on particle surfaces as well as their influence on interparticle interactions, small angle X-ray scattering experiments have been conducted at the high coherence beamline P10 at the Deutsche Elektronen Synchrotron (DESY) in Hamburg. For these experiments, dispersions of colloidal SiO_2 nanoparticles in methoxypropyl acetate (MPA) containing high molecular weight dispersants were used as model systems. Thereby, the dispersants used consist of a pigment affine core which is modified with stabilizing side chains. In order to study the structure – performance relationship of these molecules, dispersants with different degrees of modification have been used as schematically sketch in figure 1.

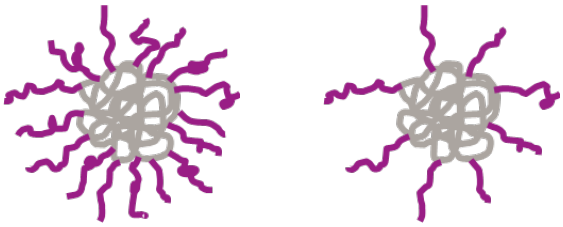

Figure 1: Schematic drawing of the molecular architecture of the dispersants used for the scattering experiments. In detail, dispersants with two different degrees of modification have been used: Dispersant A = high degree of modification (left); Dispersant B = low degree of modification

The scattering curve obtained for a pure dispersion of SiO_2 particles in MPA containing no dispersant is shown in figure 2. Here, the scattering intensity is plotted semilogarithmically as a function of the scattering vector q which is given by

$$q = \frac{4\pi}{\lambda}\sin\left(\frac{\theta}{2}\right) \tag{1}$$

with λ being the X-ray wave length and θ being the scattering angle. From the combination of eq. (1) with the well-known *Bragg's law*

$$n_B \cdot \lambda = 2d \sin\left(\frac{\theta}{2}\right) \tag{2}$$

where d is the structural length scale and n = every integer, the following fundamental relation between d and q is revealed (for $n_B = 1$):

$$q = \frac{2\pi}{d} \tag{3}$$

From eq. (3) it becomes directly obvious that q is nothing else than an inverse length whitch is proportional to d^{-1}.

The scattering curve shown in figure 2 exhibits the typical features of scattering spectra from interacting spherical colloids. Thus, for low values of the scattering vector q, *i.e.* at q-values which correspond to large length scales, a rather high scattering intensity can be observed which steeply decays with increasing q. When q reaches values that approximately correspond to the radius R_0 of the scattering particles ($q \sim \pi/R_0$), oscillations of the scattering intensity can be observed. Here, these oscillations at intermediate and high q-values are smeared out due to polydispersity effects. At very high q-values, the scattering intensity levels off approaching the incoherent scattering background.

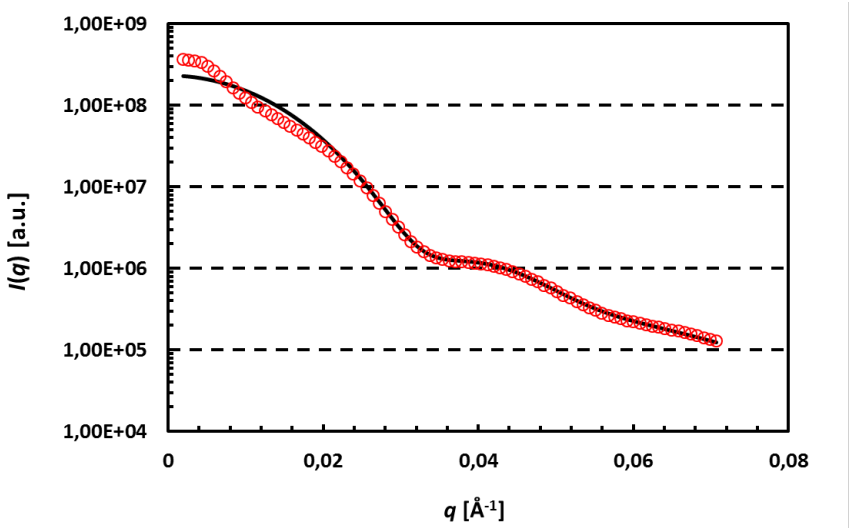

Figure 1: Scattering spectrum obtained for SiO_2 particles dispersed in MPA containing no dispersants. The data were fitted with a form factor for polydisperse, homogeneous spheres.

For the evaluation of the scattering data, the widely used decoupling approximation has been applied after which the scattering intensity can be factorized into *inter-* and *intraparticle* scattering contributions. Thus, $I(q)$ can be expressed as

$$I(q) = n \cdot P(q) \cdot S(q) \tag{4}$$

where n is the particle number density. In eq. (4) $S(q)$ is the so-called *interparticle* structure factor, which describes scattering contributions arising from interference of scattered X-rays form different particles. Thus, it is related to local correlations of different particles due to their interactions. $P(q)$ is the particle form factor which is related to the shape of the scattering particles. Mathematically it is defined as the *Fourier* transform of the electron density distribution function $\Delta\rho(r)$ describing the particle in real space.

In order to quantitative evaluate the experimental scattering data shown in figure 2 a form factor for polydisperse, homogenous spheres with sharp interfaces $P_S(q)$ was chosen. Thereby, a *Gaussian* size distribution of the particles was assumed. The two

free fit parameter of this model are the mean particle radius R_0 as well as the width of the size distribution σ. Using this model, a mean particle radius of R_0 = 124 Å with a polydispersity index $p = \sigma / R_O$ = 0,17 was obtained from the fit of the scattering data. These values are in good agreement with the information provided by the manufacturer of the silica particles.

While the medium and high q–regime of the scattering spectrum are almost quantitatively described by $P_S(q)$, significant deviations between the calculated and experimental scattering curve can be observed at large q–values, *i.e.* at large length scales. Of course, these deviations can be related to *interparticle* scattering contributions which were so far neglected. This finding becomes even more pronounced when the *interparticle* structure factor $S(q)$ is extracted from the experimental scattering data. Using equation (4), $S(q)$ can easily be calculated via:

$$S(q) = \frac{I_{\mathrm{exp}}(q)}{n \cdot P_{\mathrm{calc}}(q)} \tag{5}$$

Figure 3 shows the structure factor calculated accordingly.

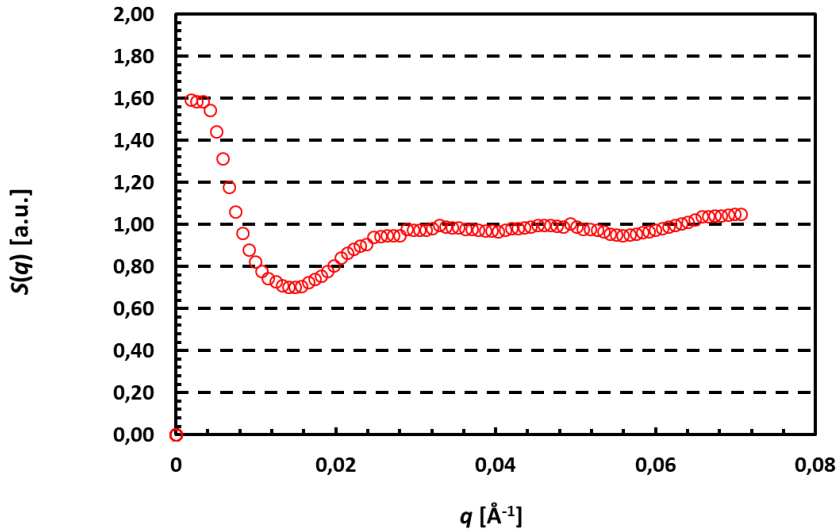

Figure 3: Interparticle structure factor $S(q)$ of a pure SiO_2–particle dispersion in MPA extracted from the experimental scattering data.

As can be seen, $S(q)$ starts at a value >1 at low q-values, runs through a minimum at $q \sim 0.01$ and then levels off to $S(q) = 1$ at high q-values. Please note that $S(q)$ would be unity over the entire q-range in case of a non-interacting system. This shape of the interparticle structure factor is very characteristic for particles with attractive interactions. Hence, the pure SiO_2-particle dispersion is only insufficiently stabilized which is also reflected in the rather poor storage stability of this system.

Starting from the pure SiO_2-particle dispersion, in a next step different amounts of Dispersant A (high degree of modification) were added to the dispersion in order to identify its influence on the interparticle interactions. Figure 4 shows the scattering curves obtained for this system for five SiO_2 to dispersant ratios ranging from 1:0 to 1:1.

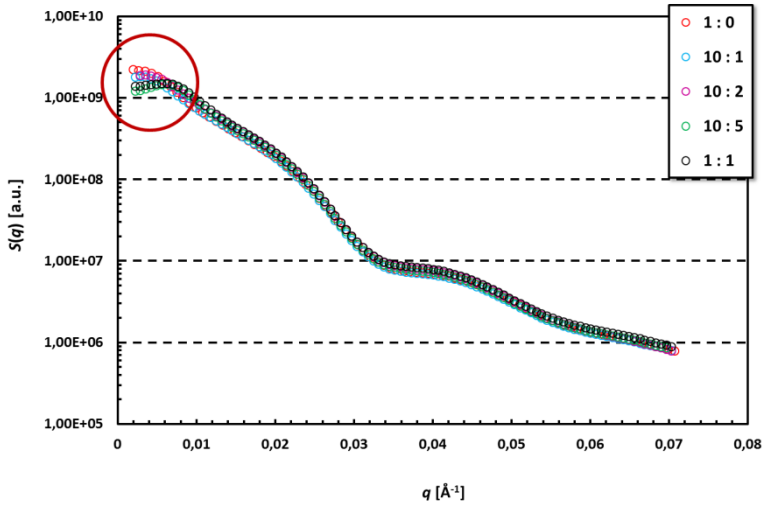

Figure 4: Scattering spectra obtained for the system SiO_2 – Dispersant A in MPA for different SiO_2 to dispersant ratios.

From these data it can be clearly seen that the addition of dispersant to the dispersion of colloidal SiO_2 significantly influences the scattering intensity at low q-values, while no variations can be observed at intermediate and high q-values. Thus, also the oscillations of the scattering intensity at

intermediate q-values whose position is directly related to the size of the scattering particles remain unaltered upon the addition of the dispersant. On a first glance this finding would imply that the size of the scattering particle does not change with increasing dispersant concentration, which in turn would mean that the dispersant does not adsorb at the surface of the SiO_2 particles. although this was already doubtlessly proven in extensive DLS measurements (not shown in this report). Additional SAXS-measurements on the pure dispersant, however, revealed that this observation is a result of a rather low scattering contrast of the dispersant molecules relative to the SiO_2 particles. Due to this low contrast, the presence of the dispersant layer remains invisible for the X-ray beam.

In order to highlight the influence of the dispersant on *interparticle* interactions, the individual structure factors were extracted from the experimental scattering spectra using eq. (5). Figure 5 summarizes the results obtained.

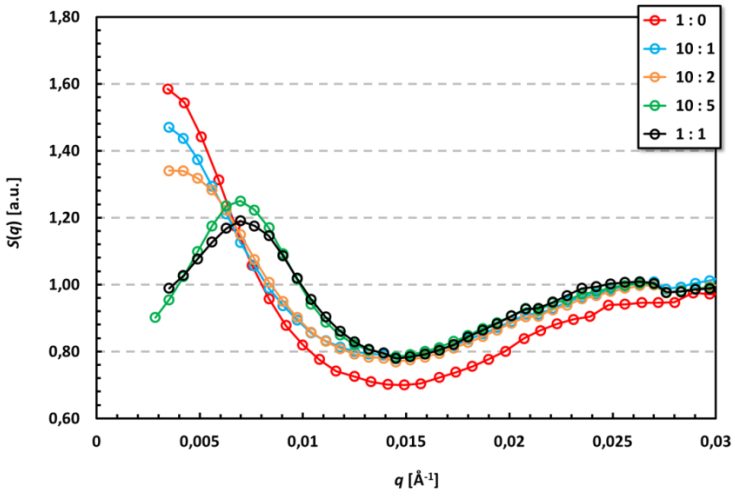

Figure 5: Interparticle structure factor $S(q)$ of the system SiO_2 – Dispersant A in MPA for different SiO_2 to dispersant ratios. $S(q)$ was extracted from the experimental scattering data using eq. (5).

From figure 5 two main trends can be identified. Thus, on the one hand, the values of $S(q)$ at $q \rightarrow 0$ steadily decrease with

increasing dispersant concentration, while the development of a pronounced maximum at around q = 0.0075 can be observed. These findings can be interpreted such that with increasing dispersant concentration attractive interaction between the scattering particles are damped (decrease of $S(q)$ at $q \rightarrow 0$). On the other hand, repulsive interactions are induced at higher dispersant concentrations (development of the maximum at q = 0.0075). These findings would strongly hint to a steric stabilization of the silica nanoparticles by the dispersant. In order to extract additional quantitative information on how the dispersant influences the interaction potential between the particles, a numerical evaluation of the individual structure factors will be performed within the next weeks.

With the aim to gain more information on the structure – performance relation of the dispersants, a second set of experiments was performed with a structural derivative of this class carrying a lower number of stabilizing side chains (*i.e.* the Dispersant B). For these experiments, the same silica nanoparticles have been used as for studies on the system SiO_2 – Dispersant A. In figure 6 the *interparticle* structure factor $S(q)$ of the system SiO_2 – Dispersant B is shown for 5 different SiO_2 to dispersant ratios. Again, $S(q)$ was extracted from the experimental scattering data using eq. (5).

From the comparison of figures 5 and 6, one dramatic difference between the Dispersants A and B can be observed. Thus, at low dispersant concentrations, *i.e.* at a silica to dispersant ratio of 10 : 1, a strong increase of $S(q)$ at $q \rightarrow 0$ can be observed for the system SiO_2 – Dispersant B, while in case of Dispersant A $S(q)$ already decreases in this q–region. This finding would hint to the fact that in the low concentration regime Dispersant B leads to an enforcement of attractive interactions between the scattering particles rather than to a steric stabilization of the system. In line with this interpretation, a macroscopic phase separation of the respective sample could be observed (see figure 6, right). Nevertheless, for high dispersant concentrations also for this

system a considerable decrease of $S(q)$ in the low q-regime as well as the development of a pronounced maximum at larger q-values can be observed. Hence, also for this system repulsive interactions between the scattering particles are induced for larger SiO_2 to dispersant ratios, *i.e.* the system is sterically stabilized in the high concentration regime.

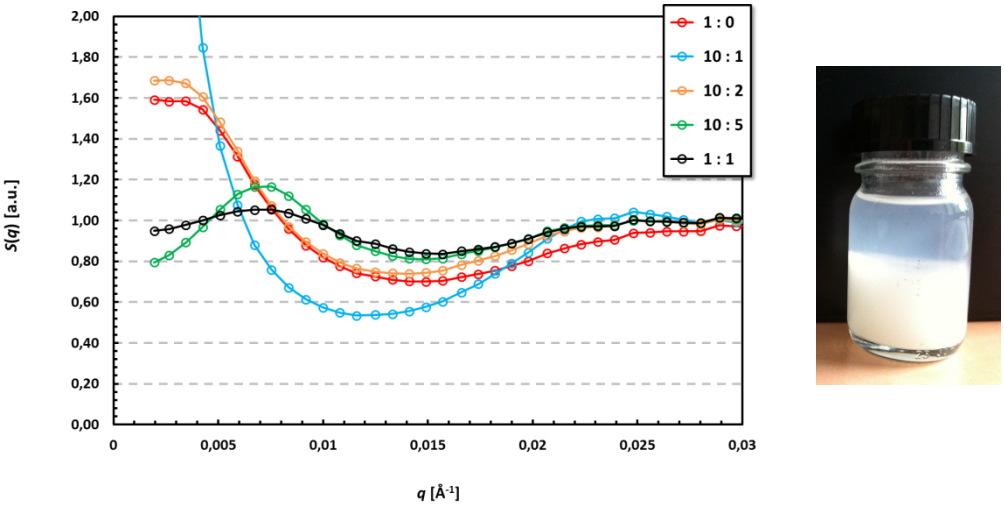

Figure 6: Left: Interparticle structure factor $S(q)$ of the system SiO_2 – Dispersant B in MPA for different SiO_2 to dispersant ratios. $S(q)$ was extracted from the experimental scattering data using eq. (5). Right: Photo of the sample at a SiO_2 to dispersant ratio of 10 : 1.

One possible explanation for these findings would be that due to its low degree of esterification, the Dispersant B leads to a bridging flocculation of the SiO_2-particles in the low concentration regime. Because of the low numbers of stabilizing side chains attached, in this dispersant the pigment-affine core is accessible for more than one SiO_2 particle and hence at low concentration these bridging effects are dominant. Only after all SiO_2 particles are sufficiently saturated with dispersant molecules, repulsive hard sphere interactions become predominant and a steric stabilization of the SiO_2 particles by the dispersant is possible. This behavior is schematically illustrated in figure 7.

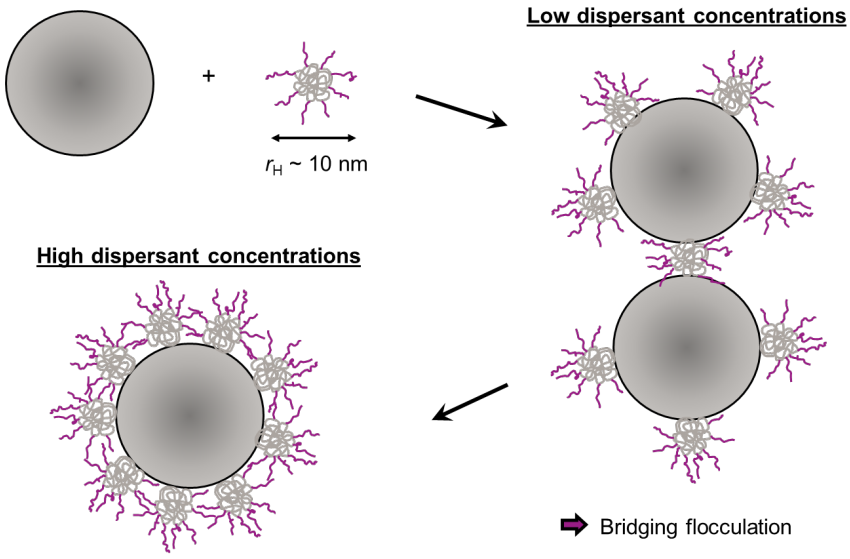

Figure 7: Schematic illustration of the mode of action of the Dispersant B in a silica nanoparticle dispersion.

In order to further support this hypothesis, application tests with Dispersants A and B in technically relevant particle dispersions have been conducted. Here it turned out that the formulation containing Dispersant B had a significantly higher viscosity. In addition, only for these formulations a yield point could be observed. Both observations are in good agreement with the interpretation of the scattering results.

In order to investigate whether a further stabilization of the colloidal silica dispersion can be achieved by a further increase in the dispersant level, additional SAXS measurement have been performed on the two systems SiO_2 – Dispersant A and SiO_2 – Dispersant B, respectively, at a silica to dispersant ratio of 2 : 10. The *interparticle* structure factors obtained in these experiments are presented in figure 8. Most surprisingly, it turned out that at such high dispersant concentrations an additional attractive interaction between the silica particles can be observed which is reflected in the strong increase of $S(q)$ in the limit $q \rightarrow 0$ as well as the absence of the maximum at larger q–values.

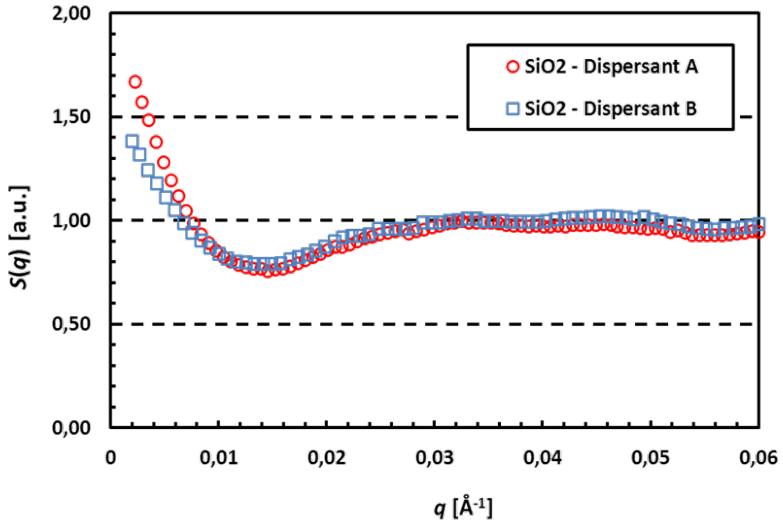

Figure 8: Structure factor $S(q)$ of the systems SiO_2 – dispersant at a silica to dispersant ratio of 2 : 10.

One plausible explanation for these findings could be as follows: In the very high concentration regime, the surface of SiO_2 nanoparticles is completely saturated with dispersant molecules and hence free, non-adsorbed dispersant molecules can coexist with nanoparticle – dispersant aggregates. These free dispersant molecules can now introduce an attractive well in the interaction potential of the particles because they are expelled from the region between two colloidal particles when their surface separation becomes smaller than the size of a single dispersant. This so-called depletion effect leads to an unbalanced osmotic pressure difference pushing the colloidal particles together, which results in an effective attraction between the particles (see schematic illustration in figure 9).

This hypothesis is further supported by the finding that in technically relevant particle dispersion containing these dispersants an unusually strong viscosity increase can be observed when very high concentrations of the dispersant are used.

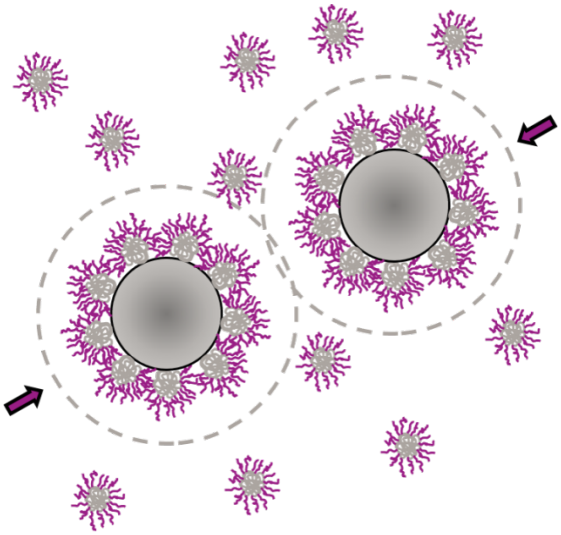

Figure 9: Schematic illustration of the mechanism of polymer-induced depletion flocculation of a colloidal dispersion.

Next steps: From the first evaluation of the scattering data, valuable information could be obtained on how dispersant molecules influence the interactions between dispersed particles. In future studies, we plan to evaluate the scattering data of systems containing dispersants with different lead structures to learn more about the structure/performance relation of these molecules.

In addition, it is planned to quantitatively evaluate the *inter-particle* structure factors in order to directly extract the interaction potential form the experimental scattering data. On the basis of the results obtained so far, it is likely that the interaction potential between SiO_2 nanoparticles in the presence of dispersant molecules takes the following functional form:

$$U(r) = \begin{cases} +\infty & r \leq \sigma \\ U_a(r) + U_s(r) & r \geq \sigma \end{cases} \quad (6)$$

Here $U_a(r)$ is the partial potential describing attractive interactions between the particles while $U_s(r)$ describes steric repulsions induced by the dispersant. Eq. (6) is based on the assumption that

the pure SiO_2 particles are impenetrable and hence $U(r \leq \sigma) = \infty$ where σ is hard core interaction radius of the particles. Using the mean spherical approximation (MSA), which is a pertubative treatment of the *Percus–Yevick* equation, the direct correlation function $C(r)$ of the SiO_2 nanoparticles can be calculated. Under the MSA one obtains

$$C(r) = \begin{cases} C_{HS}(r) & r \leq \sigma \\ -\dfrac{[U_a(r) + U_s(r)]}{k_B T} & r \geq \sigma \end{cases} \tag{7}$$

where $C_{HS}(r)$ is the known correlation function for a hard sphere system. With equation (7) one can now calculate the *Fourier* transform of $C(r)$ into q–space according to

$$\begin{aligned} C(q) &= \int_0^\infty C(r) r^2 \frac{\sin(qr)}{qr} dr = \\ &= C_{HS}(q) + \int_\sigma^\infty \frac{-U_a(r)}{k_B T} r^2 \frac{\sin(qr)}{qr} dr + \int_\sigma^\infty \frac{-U_r(r)}{k_B T} r^2 \frac{\sin(qr)}{qr} dr \end{aligned} \tag{8}$$

Inserting eq. (8) in the well–known relation

$$S(q) = \frac{1}{1 - nC(q)} \tag{9}$$

one can finally calculate the interparticle structure $S(q)$ on the basis of the interaction potential between the particles.